ALMA MATER STUDIORUM - UNIVERSITY OF BOLOGNA

SCHOOL OF ENGINEERING AND ARCHITECTURE

Second Cycle Degree in
Telecommunications Engineering

Master Thesis in

Hybrid ray-tracing/numerical methods for human exposure
evaluation for wireless power transfer wearable devices

Author:
Girish Satya Bhargav Papolu

Supervisor:
Prof. Ing. **Marina Barbiroli**
Prof. Ing. **Franco Fuschini**

To my dear parents, & my beloved brother

Contents

Nomenclature

β Electrical Allowability

BFC   Bio Fuel Cells

BS   Base Station

CMOS   Complementary Metal Oxide Semi Conductor

CNS   Central Nervous System

CPU   Central Processing Unit

DoA   Direction of Arrival

DS   Diffuse Scattering

E-Filed   Electric Field

EH   Energy Harvester

EMF   Electro Magnetic Field

ER   Effective Roughness

FDTD   Finite Difference Time Domain

FE   Finite Element

FEI   Frequency Estimation

GHz   Giga Hertz

I   Conductivity

ICNIRP   International Commission on Non-Ionizing Radiation Protection

ICRP International Commission on Radiological Protection

IEC   International Electro-technical Commission

IEEE Institute of Electrical and Electronics Engineers

IoT   Internet Of Things

meV   Milli Electron Volt

MIMO Multiple Input Multiple Output

mm   Milli Meter

NIP   Non-Ionizing Radiation

OCV   Open Circuit Voltage

PCE   Power Conversion Efficiency

psSAR Peak Spatial Specific Absorption Ratio

PV Cells Photo Voltaic Cells

RF   Radio Frequency

RT   Ray Tracing

SAR   Specific Absorption Ratio

SNR   Signal to Noise Ratio

SSC   Standard Coordinating Committee

TEGs   Thermo Electric Generators

UE   User Equipment

UHF   Ultra High Frequency

USB   Universal Serial Bus

UT   User Terminal

UTD   Uniform Theory of Diffraction

W/Kg   Watt/Kilogram

W/m^2 Watt Per Meter Square

WPT Wireless Power Transfer

List of Figures

List of Tables

Abstract

Wearable Medical Devices are assisting in the definition of fitness optimization for users. As well as health experts by gathering data that are then sent from wearables to linked devices like smartphones. With the increasing occurrences of these scenarios, data hub have been set via activity monitors that builds direct ties between patients, hospitals, pharmacies, physicians, carers, and life sciences organizations.

The scope of transmitting electrical energy without the need of cables as a physical link is known as wireless power transfer. Wireless power use the same electromagnetic fields and waves as wireless communication equipment. For wireless power transfer, many radio-frequency (RF) methods are utilized.

In this Context, the aim of this thesis is to analyze the effect of the environment in received power levels and absorbed energy inside the human body i.e. wearable devices at mm waves (e.g. 24 GHz). To this aim a RT tool, suitable for the analysis of field strength levels in the environment been equipped with a Numerical model providing SAR values inside the human body.

The elaborate is divided in five chapters: the first one highlights the main characteristics of the Wearable technologies and its feeding techniques. In the second chapter, a detail description of the Exposure Limits and assessment techniques; in the third chapter the main features of Ray Tracing and Numerical Methods are discussed; in the fourth chapter models and methodology with particular emphasis on the Hybridization of Ray-tracing along with Numerical Methods for optimizing the desired Output are shown. Chapter five presents the output data we have achieved and Finally, chapter six concludes this work.

Chapter 1

Introduction

Wearable wireless communication systems hold great promise for their rich potential in diverse areas (e.g., medical monitoring, firefighter tracking, wearable computing, and battlefield survival, etc.) eliciting considerable research interest and industrial investment over the past decade.[4]

Over the years, wearable sensors have attracted considerable attention due to their ability to offer constant and real-time physiological information. Their work in measuring dynamically and non incisively biochemical markers can be found in biological fluids which includes sweat, tears and interstitial fluids. Recently the non-invasive monitoring of bio markers through the use of biosensors for the healthcare and sports analytic has gained interest of many researchers .

However, they need appropriate energy sources with their maintenance depending on a continuous, stable and sufficient supply of power, as different forms and applications of wearable sensors need different levels of energy to work.

1.1 What Is Wearable Technology?

Wearable technology, also known as "wearables", is a classification of electronic devices that can be worn as accessories, embedded in clothing, implanted in the user's body, or even tattooed on the skin. The devices are hands-free gadgets with practical uses, powered by microprocessors and enhanced with the ability to send and receive data via the Internet.[5]
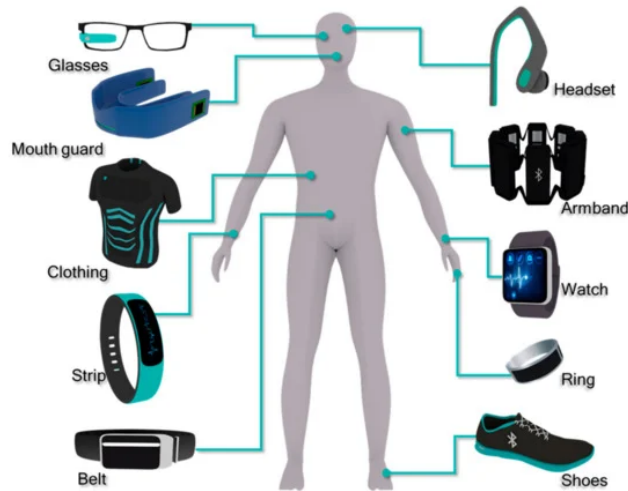
Figure 1.1: Wearable devices

[6]

1.2   How wearable technology has evolved throughout the decades

- In 1950's, Wearable tech [7] began very differently from today's recognisable devices, with Sony's first transistor radio making its debut in 1955."The Sony TR-55 served as the template for portable gadgets we use today. Everything from the IPOD to the Game Boy can trace its basic handheld design to the TR-55's form factor."- Wired Magazine.

- 1970s Wearable tech [7] went mainstream in 1975, as the first calculator wristwatch was released. Worn by Sting on the cover of the Police's Wrapped Around Your Finger, and by Marty McFly in Back to the Future, it become an icon of the 70's and 80's.

- 1980s The WALKMAN [7], launched in 1979, became out go-to music device throughout the 1980's.A revolution in music and wearable technology, the Walkman was so popular it sold over 200 million units. "Don't you think a stereo cassette player that you can listen to, while walking around is a good idea!" Sony Chairmen, Akio Morita. In 1987, digital hearing aids were released, revolutionizing the healthcare industry.

- 1990s In December 1994 [7], Steve Mann, a Canadian researcher, developed the Wearable Wireless Webcam. Despite its bulk, it paved the way for future

IoT technologies. Wearable technology conferences and smart clothing expo began to see a rise in popularity throughout the decade.

- 2000s Wearable technology found its groove in the 2000s [7], with the introduction of Bluetooth headsets, the Nike iPod, Fitbits, and many more.

- 2010s The Wearable craze [7] exploded in 2013, Google Glass entered the market, followed by the Apple Watch in 2015, and the Oculus Rift Headset in 2016. Today, clothing designers are experimenting with fabrics and technology, signalling that smart clothing is on its way to the mainstream. Some innovative items are already available, like the Nadi X Yoga Pants, which feature in-built haptic vibrations to encourage you to move or hold positions. [7]

1.3 Wearable devices feeding techniques

Wearable sensors have strong potential for improving current medical systems[8], as they are able to provide extensive monitoring of various physiological functions and highly efficient economical services in a variety of fields. However, wearable sensors need appropriate energy sources, given that their maintenance depends on a continuous, stable and sufficient supply of power. Different forms and applications of wearable sensors require different amounts of energy to work[8].

Available biosensors and wearable sensors under development require various power levels to be delivered from different sources of energy. Figure 1.2 shows some of the sources of energy that can be harvested, converted, and used to supply power to wearable sensors[8]. Energy collected from light, heat, radio waves, or vibrations can be converted into electrical energy to power wearable sensors.

1.3.1 Main feeding techniques for wearable devices

The main energy solutions for wearable sensors are reviewed in the following sections[8]:

- Batteries

- Solarcells

- Thermo electric Generators

- Kinetic Energy Harvesters

- Biofuel Cells

- Radio Frequency energy harvesters and wireless power transfer (WPT)
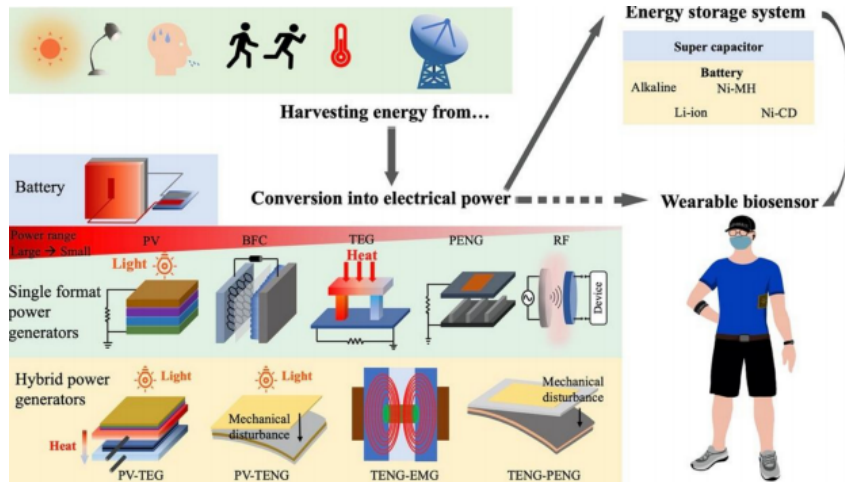
Figure 1.2: Schematic flow chart of self-powering smart wearable sensors
[8]

- **Batteries**[8]

  Powering the Wearable technologies, similar to any of the embedded system or a portable device, requires batteries. Over the period of time batteries has been developed with the aim to meet the power requirements of various wearable sensors.

Figure 1.3: Nikel Hybrid Battery
[9]

Alkaline batteries, which are being in use since the starting of the 20th century have been tested vigorously and widely used[8]. Their feature of being safe and easily replaceable have exponentially increased their popularity.

The main types of alkaline batteries are AA and AAA. These are also available in coin cells and have a 1.5 V standard voltage and an 11.6 mm diameter and 5.4 m height. However, the voltage of these batteries drop significantly with continued use, a steady and stable voltage is not achievable, and the voltage drops more significantly when they are approaching last stages of their lifespan[8].

Nickel-metal hybrids are an alternative class in batteries which can be used to power up wearable sensors. These are rechargeable and have a capacity which is three times powerful compared to the Nickel-sodium batteries, with a value approaching that of lithium-ion batteries are the most commonly used batteries for wearable sensors[8].

However the high toxicity of battery electrolytes is a major concern that cannot be ignored. On the other hand, wearable sensors have large limitations in size.

- **Solar Cells**[8]

Solar cells have been introduced to replace batteries to increase the device efficiency as well as to make it lighter. They have various benefits in maintaining wearable device functionality[8].
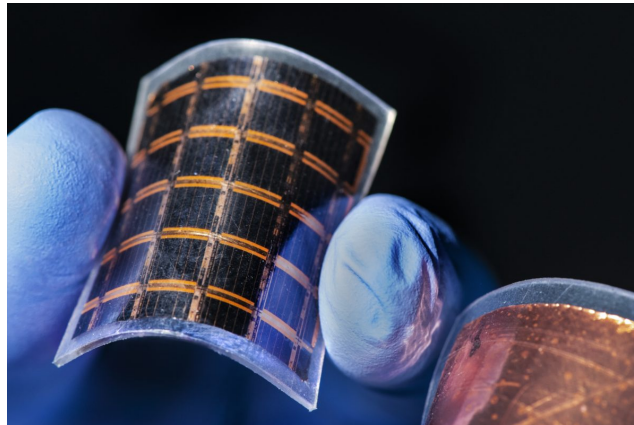
Figure 1.4: Solar cells

[10]

They can charge the wearable devices through a USB connection integrated into a piece of cloth. Since the introduction of miniaturized solar cells, it has become possible to generate power by solar energy in a variety of wearable objects.

They can also help in optimizing the energy storage modules performance and make them more stable and adaptable for a wearable device. In addition to their high flexibility and scalability, a fibre based super-capacitor can absorb and make use of sunlight energy to guarantee operation under extreme low temperatures ($0°$ C), making it a favourable choice of a combined energy harvesting and storage device for wearable biosensors.

The other class of solar cells are the Perovskite solar cells which offer a flexible, efficient and lightweight energy solution for wearable electronic sensors[8]. They are thin, flexible and favoured in portable electric chargers and wearable electronic textiles due to their convenience and versatile functionalities. Apart from being flexible, stretchable, another prominent factor that can greatly effect the performance of solar cells is light intensity. Solar cells need further enhancement to improve their indoor performance, as the weather is not controllable and users spend most of their time inside buildings.

These solar cells exhibit a higher power conversion efficiency (PCE) than those of optimized single-junction flexible organic solar cells. The most recent applications of perovskite cells based on organic light absorbing halides have shown to be economically and practically viable.

Although solar cells exhibit higher PCEs than other types of energy generators, their efficiencies of PV cells depends greatly on the type of material used. Additionally, because some textile-based solar cells may suffer severe reductions in PCE following fatigue, the mechanical properties of solar cells should also be taken seriously into account. For example, when applied to wearable devices, these flexible devices face more complex body motions compared to experimental conditions. How to avoid material failure and performance degradation has become a problem that cannot be ignored. On the other hand, the temperature of solar cells can exceed the temperature of the human body significantly.

- **Thermo-electric Generators**[8]

TEGs are one more type of energy source that can be used to power wearable devices. They are durable, produce no noise, and generate the energy needed to directly power wearable devices by converting heat into electrical energy[8].

TEGs have been proven to be effective in powering wearable sensors by using waste heat from the human body. The human body is a great portable
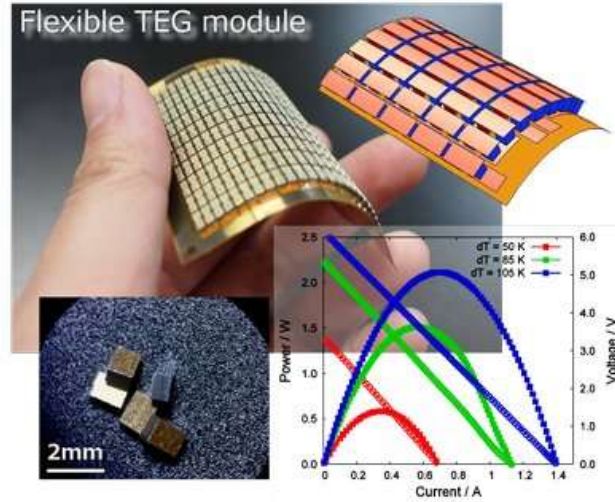
Figure 1.5: Thermo-Electric Generators

[11]

source of energy, generating up to 58.2 W/m^2 in waste heat at rest. Even a tiny portion of this waste heat is adequate to run the majority of low-energy wearable gadgets without the use of batteries as a backup energy source. TEGs can also be directly incorporated into wearable textiles.

Wearable sensors that use body heat can be used to monitor human vitals and chronic diseases over time. Human body heat-powered sensors have been utilized in hearing aids and accelerometer-based rehabilitation devices to monitor glucose levels[8].

Thermo-electric energy offers several benefits over conventional power sources for wearable sensors. The conversion of mechanical energy into electrical energy necessitates the user's active participation, which may be impossible for the old or bedridden. Furthermore, when users are subjected to low-lighting situations, solar cells may fail to work correctly. TEGs, on the other hand, provide continuous power as long as there is a temperature differential between the skin and the ambient temperature, which is common for most practical circumstances.

The Seebeck effect is used by TEGs to convert heat into electrical energy [8]. When incompatible materials, such as metals or semiconductors with n-type and p-type components, have junctions at different temperatures, electron and hole carriers will migrate to the cool ends. The Seebeck effect causes

electric fields to form in both materials that are proportional to the temperature gradient. Current can flow if there is a circuit link. TEGs are formed by layering a heat sink between n- and p-type semiconductors and a heat source.

People release energy as a result of metabolic activities, which serve to keep the core body temperature stable. The body temperature necessary for people to operate normally is around 37 degrees Celsius. Heat departing the skin is transmitted to the surrounding environment by convection and radiation at a rate of 110 mW/cm^2. The rate at which heat is transported varies on the bodily component in question.

Electric generators that employ body heat as an energy source may have certain flaws due to inadequate conversion of body heat to electricity. Thin TEGs that consume less energy are required for efficient conversion. Furthermore, in some applications, flexible wristbands with TEG modules that record enough accelerometer data from a user are required.

- **Kinetic Energy Harvesters**[8]

Another form of energy source used to power wearable sensors is energy harvesters (EHs)[8].
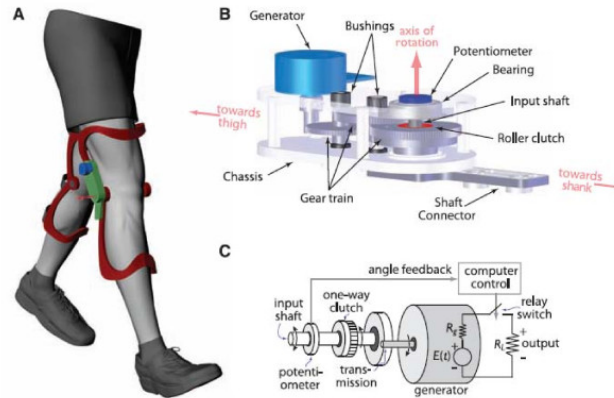
Figure 1.6: Kinetic Energy Harvesters

[12]

Kinetic Energy Harvesters work by capturing and storing vibrational energy generated by either human body motions or nature events. Because they are bio-compatible and ecologically benign, EHs are called green. EHs produce low voltages and are appropriate for low-power applications.

EH technology employs a variety of approaches. The most significant technology is kinetic energy harvesting, which converts human motion into energy. Kinetic energy harvesters employ vibration or motion to create electricity. Their transduction processes are categorized as electromagnetic, electrostatic, piezoelectric, and triboelectric.

- **Biofuel cells**[8]

BFCs are another type of energy recovery technique that is utilized in wearable sensors. A fuel cell is an electro-chemical cell that generates electricity through reactions between the chemical species flowing into the cell at the anodic site and the oxidant at the cathodic site. Fuel cells vary from traditional batteries in that they may generate continuous energy as long as the reactants are available[8].
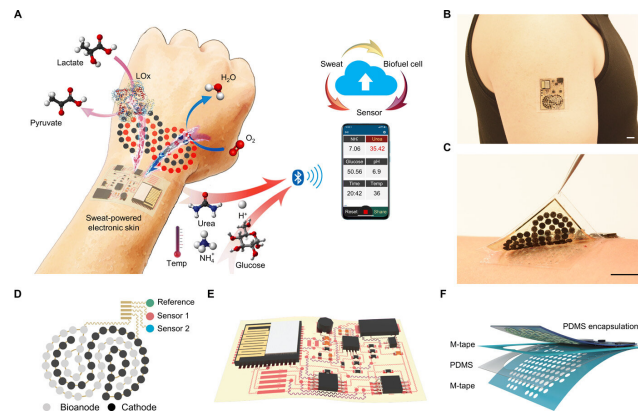
Figure 1.7: Bio-fuel Cells

[13]

While there are other types of fuel cells, the most widely used fuel cell uses a proton-exchange membrane. A membrane separates the fuel and oxidant in this form of fuel cell, enabling only protons generated at the anodic site to pass the membrane and minimizing the quantity of oxidant present at the cathodic site. Electrons produced at the anode cannot travel through the membrane to reach the cathode; as a result, they must choose another path, resulting in current production.

There are several advantages to using fuel cells to power wearable sensors. The most significant advantage is that the presence of reactants within the fuel cell eliminates the need to replace the batteries. Furthermore, elderly

or bedridden people may benefit from wearable sensors driven by BFCs that use reactants found in the human body, such as glucose or lactic acid.

When using BFCs to power wearable sensors, the power supply and biosensing can be integrated to simplify the design. Epidermal BFCs have been utilized to create energy by oxidizing lactic acid in perspiration. Sweat energy contributes to bio fuels producing ten times more energy per unit area than any other bio fuel utilized in wearable sensors.

Despite the fact that the technique had been shown to be effective in creating energy, it was impossible to determine the quantity of energy that these fuel cells could produce per unit area. As a result, there is a requirement to quantify the amount of material to be used as well as the material combination ratio, as these parameters affect the amount of power generated. Researchers are also working to improve the adaptability of biofuel cells. Few studies suggested a lactic paper-based biofuel cell that has the potential to be highly useful in wearable applications.

It has a 3.4 V open circuit voltage (OCV) with six cells in series and a 4.3 mW output power with a 6x6 cell array. Researchers presented a flexible bracelet BFC [8] that collects sweat and uses lactate to power wearable electronics. At 20 mm lactate solution, it has a maximum output power of 74 W and an OCV of 0.39 V.

The biofuel cell array has been shown to function well in terms of powering devices at a reasonable cost. In general, BFCs are highly bio compatible and have reduced manufacturing costs.

They rely on biological molecules to power wearable sensors. More BFCs with great flexibility and compact size have recently been explored. BFCs, on the other hand, require more research to improve their PCE. Their output power, on the other hand, is significantly dependent on analyte concentration.

- **Radio Frequency energy harvesters and wireless power transfer (WPT)**[8]

  Wireless power RF harvesters provide an energy solution for wireless sensor networks. RF technology extracts energy from the environment or from designated energy sources. RF harvesters are appealing for a variety of applications.

  RF harvesters, unlike other energy harvesters such as solar cells or chemical generators, provide a continuous and controlled supply of power, making
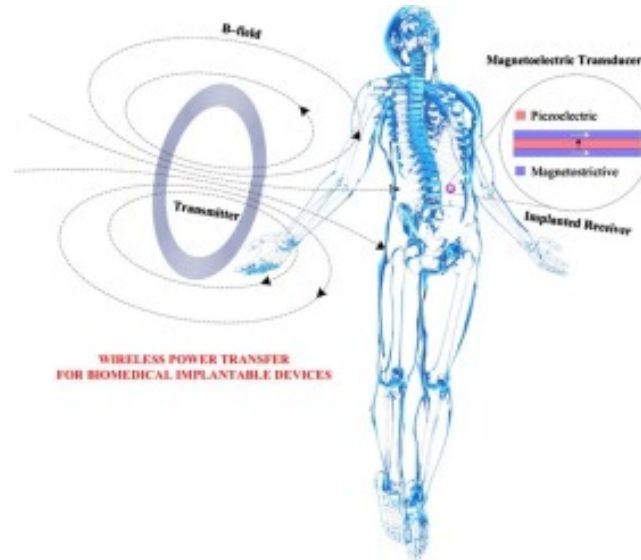
Figure 1.8: RF harvestors

[14]

them suitable for applications requiring greater amounts of energy. Furthermore, RF waves have been employed to convey wireless information in wireless communications and can be used to transmit sensor data.

RF power transfer can be classified as near-field inductive and capacitive coupling power transfer, ultrasonic power transfer, or mid- or far-field electromagnetic power transfer, depending on the WPT range. Near-field inductive coupling is an emerging technology that has been utilized to power cochlear wearables[8]. To create great power, however, precise alignments are required. To power flexible patches, near-field capacitive coupling is employed, but the related power transfer efficiency (PTE) reduces substantially when the transmitting and receiving coils are apart.

Large PTE variations impede ultrasonic energy transmission. When the frequency exceeds tens of gigahertz, mid-field and far-field RF harvesters become less efficient (GHz).

WPT and data transmission have been studied during the last few years. Because RF signaling enables both of these transfers, several researchers have studied simultaneous wireless data transmission and power transfer, which combines the two approaches[8].

There are various issues with using RF harvesters to power wearable

sensors. In nearfield systems, for example, RF energy harvesting cannot create enough power without precise alignment. Far-field RF harvester systems have a low PTE by design and may not meet the power demands of wearable devices.

One of the primary problems of RF harvesters is their capacity to supply sufficient energy. RF harvesters, on the other hand, require wake-up power since the Complementary Metal-Oxide-Semiconductor (CMOS) transistor has a threshold. Although RF energy appears to be a desired and dependable source of energy for wearable devices, there is always space for development.

1.4   The Need for exposure evaluation

The millimeter wave frequency band (mmWave) is a part of the radio frequency (RF) spectrum. It consists of frequencies between 30 GHz and 300 GHz, corresponding to the wavelength range of 10 to 1 mm. The photon energy range of millimeter wave is 0.1 to 1.2 milli electron volts (meV) is different from ultraviolet rays, X-rays and gamma rays, thus millimeter-wave radiation is non-ionizing. The main safety issue is that human body absorbs millimeter-wave energy, which leads to warming effects.[15]

Unlike ionizing radiation (ultraviolet, x-ray and gamma rays) which are associated with cancer due to electron shift during exposure, millimeter radiation is not ionizing because the energy of the photons is not sufficient to remove an electron from the atom or molecule. (typically 12 eV is required). Thus, at frequencies of the order of millimeters, the energy of the photons is more than four orders of magnitude less than ionizing radiation and therefore unable to displace electrons, breaking the molecular bonds; this disorder is associated with cancer.

Communication systems must comply with latest regulations of International Commission on Non-Ionizing Radiation Protection (ICNIRP) to prevent any adverse health effects associated with these thermal effects.

Chapter 2

Exposure limits and exposure assessment

2.1 Exposure Standards

Several scientific bodies of national and international organizations produce safety standards for exposure to electromagnetic fields. The International Commission on Non-Ionizing Radiation Protection (ICNIRP) and the IEEE's Standards Coordinating Committee 28 (SCC28) are the two most notable of these groups[16]. These committees keep a close eye on scientific publications in order to develop exposure limits based on consequences that the scientific community considers well-established. These restrictions are set forth in guidelines that are updated on a regular basis.

The ICNIRP 1998 Guidelines provide the foundation for national regulators to implement relevant legislation. The Latest ICNIRP 2020 enacted the minimum requirements for the protection to safeguard People from the harmful effects of electromagnetic field, which is enforced by national law[16].

There are two types of exposure limits defined by safety guidelines:

- The basic restrictions

- The reference levels or the maximum permissible exposure.

Physical quantities that are closely connected to radio frequency-induced ill health consequences are the subject of "Basic Restrictions". Some of these are physical quantities inside an exposed body that are difficult to quantify, thus "Reference

Levels" have been created from the fundamental limits to give a more practical way
of confirming compliance with the standards.

Basic restrictions and differences with 1998 values

Parameter	Freq. range	ΔT	Spatial	Aver. time	Health effect level	RF	Occup.	RF	General public
Core ΔT	100 kHz-300 GHz	1°C	WBA	30 min / 6 min	4 W/kg	10	0.4 W/kg	50	0.08 W/kg
Local ΔT (Head & Torso)	100 kHz-6 GHz	2°C	10 g	6 min	20 W/kg	2	10 W/kg	10	2 W/kg
Local ΔT (Limbs)	100 kHz-6 GHz	5°C	10 g	6 min	40 W/kg	2	20 W/kg	10	4 W/kg
Local ΔT (Head, Torso, Limbs)	>6-300 GHz / 30-300 GHz / 10-300 GHz	5°C	4 cm² / 1 cm² / 20 cm²	6 min / 6 min / $68/f^{1.05}$	200 W/m² / 400 W/m²	2	100 W/m² / 200 W/m² / 50 W/m²	10	20 W/m² / 40 W/m² / 10 W/m²
Pain (contact current)	100 kHz-110 MHz (*guidance* level / reference level)	--	--	10 sec	20/10 mA (adult/child)	1	20 mA / 40 mA	1	20/10 mA (ad./child) / 20 mA

8   Eric van Rongen

Figure 2.1: ICNIRP Guidelines 1998 Vs 2020

[14]

Overcoming these limits can have health consequences, and that's why there are
limitations (including a safety factor). Tissue heating can result from RF energy
absorption over 100 kHz or nerve activation from contact currents or generated
currents or fields in the body below 10 MHz[16]. In order to avoid thermal stress
and local thermal damage, the RF energy absorption is restricted by the specific
absorption rate (SAR) averaged across the whole body. Below 10 MHz, the induced
fields are further restricted to avoid damaging nerve tissue.

In terms of current density or averaged electric fields, these limitations are set
when enough nerve cells are considered. When it comes to developing WPT systems,
safety is always a top priority[16], and one of the most critical safety variables to
consider is SAR. SAR is a unit of power absorbed per kilogram of mass (W/kg) that
has been the subject of much research to assure human safety. A high SAR and
Incident Power Density can be harmful to human health because biological tissues
absorb heat and elevate body core temperatures to dangerous levels, especially at
radio frequencies (RF).

	Whole body SAR	Partial body SAR	Head SAR	Local SAR (a)		
Body Region →	whole body	exposed body part	head	head	trunk	extremities
Operating Mode ↓	(W/kg)	(W/kg)	(W/kg)	(W/kg)	(W/kg)	(W/kg)
Normal	2	2–10 (b)	3.2	10 (c)	10	20
1st Level Controlled	4	4–10 (b)	3.2	20 (c)	20	40
2nd Level Controlled	>4	>(4–10) (b)	>3.2	>20 (c)	>20	>40
Short duration SAR	The SAR limit over any 10 s period shall not exceed two times the stated values					

Figure 2.2: Basic Restrictions on SAR in Watts per kilogram According to Exposure Guidelines[1]

$$SAR = \frac{1}{V} \int_{sample} \frac{\sigma(r)|E(r)|^2}{\rho(r)} dr \qquad (2.1)$$

Where σ is the sample electrical conductivity, E is the RMS electric field, ρ is the sample density, V is the volume of the sample[16]. The International Commission on Non-Ionizing Radiation Protection (ICNIRP 2020) and the Institute of Electrical and Electronics Engineers have produced standards for RF exposure. Local SAR is defined as the power absorbed per 10-g cubical mass, according to ICNIRP and IEEE recommendations.

PROTOCOL	BODY REGION	FREQUENCY	E-FIELD
ICNIRP 1998	CNS of the head and body	100KHz−10MHz	
ICNIRP 2010	all	3kHz−10MHz	$1.35 \times 10^{-4} \ f_H$
IEEE 2015	brain	20kHz−5MHz	$2.95 \times 10^{-4} \ f_H$
	heart	167Hz−5MHz	$5.65 \times 10^{-3} \ f_H$
	extremities	3.35kHz−5MHz	$6.27 \times 10^{-4} \ f_H$
	other	3.35kHz−5MHz	

Table 2.1: Basic Restrictions on the SAR in Watts per Kilogram According to the Exposure Guidelines[3]

Peak-spatial SAR (psSAR) is the maximal SAR and should be researched for our WPT system since it only radiates in a limited region of the human body; hence, local exposures are more important. Due to absorption differences across the human body, ICNIRP and IEEE impose various recommendations to different parts of the human body.

The following bodily regions are defined by the ICNIRP:

- "Head and Torso" which includes the head, eye, pinna, belly, back, thorax, and pelvis.

- "Limbs" which includes the upper arm, forearm, hand, thigh, leg, and foot.

2.2 Interaction Mechanism

Radio frequency EMFs are made up of oscillating electric and magnetic fields; "frequency" refers to the number of oscillations per second[16] and is measured in hertz (Hz). As the field moves away from a source, it transmits power from the source, which is measured in watts (W), which is equivalent to joules (J, a unit of energy) per unit of time (t). When the field collides with a substance, it interacts with its atoms and molecules. When a biological organism is subjected to radio frequency EMFs, part of the energy is reflected away from it, while the rest is absorbed. As a result, inside the body, complex patterns of electromagnetic fields emerge that are significantly influenced by EMF characteristics as well as the physical features and dimensions of the body. The electric field is the most important component of the radio frequency EMF that affects the organism.

Induced electric fields (E_{ind}, measured in volts per meter[16], Vm^{-1}) are electric fields that exist inside the body and can impact the body in a variety of ways that are potentially harmful to health. To begin with, the generated electric field in the body acts on both polar molecules (mostly water molecules) and free-moving charged particles such as electrons and ions. A portion of the EMF energy is transformed to kinetic energy in both circumstances, causing the polar molecules to spin and the charged particles to flow as a current. As polar molecules and charged particles spin and travel, they often interact with other polar molecules and charged particles, converting kinetic energy to heat.

This heat may harm your health in a variety of ways[16]. Second, if the applied electrical field is powerful sufficiently and below about 10 MHz, it can stimulate nerves, and if the applied electrical field is powerful and brief enough (as can be the case for pulsed low frequency EMFs), it can cause dielectric breakdown of biological membranes, as happens during direct current (DC) electroporation.

Simplified anatomical models are used to create these reference levels, which conservatively link incident field levels with the basic limitations. Additional steps must be required to demonstrate compliance with safety limitations when incident fields

exceed reference levels. Direct measurements of the SAR or numerical simulations of the SAR or generated currents utilizing anatomical high-resolution human body models are examples of these measurements.

2.3 Reference Levels

These are EMF exposure values outside of the human body, calculated using basic constraints in worst-case scenarios[16]. These EMF exposure limits are produced from a mixture of measurement and computational investigations, and are used to compare the values of physically measurable physical quantities. Some of the measured values for reference levels are magnetic flux density, magnetic field strength, electric field strength, power density, Specific Energy Absorption, and contact currents. These values are measured and compared to comparable reference levels in a specific EMF exposure circumstance.

To create reference levels based on RF, several assessment rules are framed. Reactive near-field, far-field, and radiative near-field EMFs exist. The reference level recommendations are more cautious than the equivalent basic constraints, and they are developed by taking into account uncertainties in EMF source type, physical dimension, and changes of EMFs in the space inhabited by a human body.

2.4 Compliance Testing Standards

As of yet, there are no product standards or particular methods for measuring and numerically evaluating human electromagnetic exposure that satisfy the demands of wireless power transmission systems. Portable wireless devices operating in the 30 MHz to 6 GHz frequency band have SAR measuring standards defined.

These norms provide dosimetric phantoms and equipment requirements for determining the SAR directly. WPT's frequency range does not lie within the reach of these standards, and specially created phantoms and tissue simulants preclude its easy expansion to lower frequencies. International Electrotechnical Commission (IEC) standards on the measurement of electromagnetic fields of household appliances and on the assessment of electrical equipment related to human exposure describe methods for quantifying incident fields and provide generic methods for assessing compliance with basic restrictions.

There is a difference between the scope of Assessment of human exposure to EM fields from WPT systems[3] (which is restricted to 400 kHz) and the scope of

Assessment of electronic and electrical equipment related to human exposure[17] (which covers WPT). Nevertheless, it merely proposes useful and extremely general methods for evaluating human body currents, E-fields, or SAR. Since it lacks the repeatability and precision needed for devices that might potentially expose users to exposure levels comparable to or above the basic limits, it cannot be considered adequate.

For situations when experimental approaches fail to provide the needed degree of detail or precision, regulatory agencies have encouraged the use of measurements combined with numerical models. Technical guidelines for the proper use of numerical techniques in compliance testing are being developed.

2.5   Exposure Mechanism

It depends on the operating frequency and application on how wireless power transmission devices affect human body[16]. Between several hundred megahertz and several gigahertz in frequency, both electric and magnetic fields are involved in the danger.

Anatomical changes in tissue thickness and dielectric properties of the exterior layers (skin, fat and muscle) are sufficient for a simple conservative assessment of the local SAR with regard to worst-case coupling and local field enhancements.

Such an analysis can be used to establish dielectric parameters for homogeneous tissue simulants or the required correction factors. Body phantoms for compliance testing at 30-300 GHz have been developed using this method.

2.6   Specific Absorption Ratio

Specific Absorption Ratio (SAR) [16] is defined as the time derivative of the incremental energy consumption by heat, δW, absorbed or dissipated in an incremental mass, δm, contained in a volume element δV of a particular tissue mass density (kg/m^{-3}), ρ, and is represented in watt per kilogram (Wkg^{-1}) :

$$SAR = \frac{\delta}{\delta t}\left(\frac{\delta W}{\delta m}\right) = \frac{\delta}{\delta t}\left(\frac{\delta W}{\rho \delta V}\right) \tag{2.2}$$

Because of the relative magnetic permeability(μ_r) is 1 , the dielectric characteristics of the biological tissues or organs are often regarded as dielectric lossy material and magnetically transparent. Therefore, the SAR is usually derived from

$$SAR = \frac{\sigma |E|^2}{\rho} \tag{2.3}$$

Where σ is the conductivity (Sm^{-1}) and E is the internal electric-field (root mean square (rms) value).

SAR is highly connected with temperature increase. SAR and temperature increase are closely connected under situations when heat loss owing to mechanisms such as conduction is not considerable.

$$SAR = C\frac{dT}{dt} \tag{2.4}$$

where C is the tissue's specific heat capacity, T is the temperature (°C), and t is the exposure time (s). In most practical instances, a considerable quantity of heat energy diffuses fast throughout the exposure.

2.7 Methods and requirements for exposure assessment

2.7.1 Anatomical Models

The dielectric characteristics of human tissues are quite variable. Muscle, brain, skin, and inner organs are all examples of tissues with high water content, while fat and bone are examples of tissues with low water content. Tissues and bodily fluids with a high water content have a permittivity between 100 and 500 at 10 MHz and a conductivity between 0.15 and 1.5 S/m [3]. There is an 8 to 36 fold variation in the relative permittivity of low water content tissues at this frequency, as well as conductivity's of 0.01 to 0.08 S/m. Nerve and muscle tissues have an-isotropic dielectric properties when compared to bone.

A good coverage of the anatomical features of the exposed population is required to estimate the local SAR since simple geometrical forms may accurately depict the human body for whole-body absorption testing.

Additionally, while constructing a body with arms, legs, or fingers, the posture should be taken into account because it has the potential to dramatically affect local absorption. Analyses of anatomical body models created for radiation dosimeter using ionizing and non-ionizing radiation.

Figure 2.3 shows virtual population models that may be moved and rotated using special software and exported in a generic data format for use with the Finite-Difference-Time-Domain(FDTD) method. New techniques for articulating the limbs of these models and altering their mass have been discovered recently.
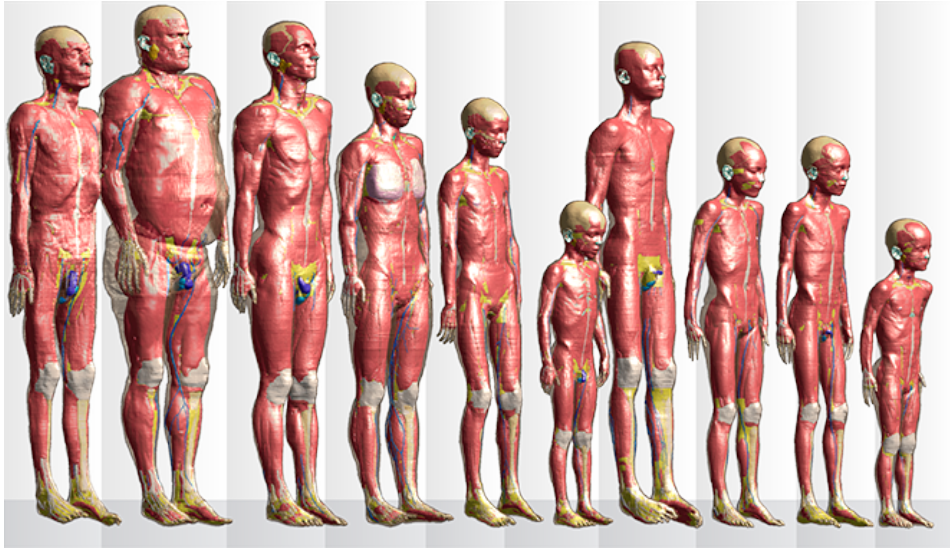
Figure 2.3: Anatomical whole-body models of adults and children of the virtual population[1]

2.7.2 Numerical Analysis Techniques

The Finite-Difference-Time-Domain(FDTD) algorithm has risen to prominence in RF dosimetry in recent years as the most used numerical approach. FDTD is a full-wave technique [3], which means it applies the first and second of Maxwell's equations to the problem it can readily produce dielectric forms as complicated as a human body anatomy model.

Additionally, the unfavorable relationship between the typical frequency of operation of wireless power transmission systems[3] and the time step limit necessitates lengthy simulation times in order to reach steady state (if the simulated system is driven by a sinusoidal signal) or to let a transient die away (if the system is excited by a broadband pulse).

With the Finite element (FE) technique, full-wave and quasistatic solutions to Maxwell's equations may be calculated. Methods that use the frequency domain and do not have a time step restriction are known as Frequency Estimation (FEI). Model creation becomes problematic when simulating complicated dielectric structures [3] such as an anatomical body model using FE, which is generally done on tetrahedral grids.

Anatomical body models should be able to discriminate between distinct tissue layers with differing dielectric characteristics, such as the skin and the subcutaneous fat [3]. New versions are presently being created. Finite element (FE) or a com-

bination of the method of moments (MoM) with either FE or boundary element techniques can produce great computing efficiency for body models with homogeneous tissue distribution, such as the experimental phantoms described in.

A quasi static approximation may be used to evaluate the anatomical models' dosimetric performance because the WPT's free-space wavelength is many tens of meters. Testing if the quasi static approximation is valid requires the following conditions to be met:

$$|k^2 D^2| << 1 \qquad (2.5)$$

with

$$k^2 = \omega(\omega\epsilon + j\sigma)\mu_0 \qquad (2.6)$$

where k is the medium's wave number. k is related to the wavelength λ by the formula k $= 2\pi$, ϵ and σ represent the permittivity and conductivity of the body tissues [3], respectively, while μ_0 represents the permeability of free space. D represents the diameter of each relevant region of the computational domain.

Quasistatic methods have been implemented as a special variant of the FE method utilizing finite-difference approximation [3]. It's simple to show that equation 2.5 isn't always met in common exposure scenarios to wireless power transmission systems and should be examined before using a numerical technique.

There is almost no difference in the magnetic field while the body is in it. As a result, the magnetic field of a wireless power transmission system may be distinguished from the person who is subjected to it. Dosimetric values may be simulated in a human body model using incident fields.

2.7.3 Experimental Methods

If the exposure is in the near field, the source model is complicated, or the properties of the source are affected by the presence of a human body, measurements are preferred over numerical models. Although numerical simulations are better at anatomical modeling [3], the results might be affected by the model's underlying features (such as dielectrics and manufacturing tolerances). Wireless communication technologies (such as mobile cellphones), base stations, and magnetic resonance imaging systems all have standardized measuring techniques for human exposure, while WPT does not.

The ideas of scientifically sound measuring techniques that lead to a conservative estimate of human exposure are defined here. Frequencies below 10 MHz and tissue

heating processes are part of the WPT's focus range (above 100 kHz)[3]. Since both induced fields (such as an electric field or current density) and SAR must be assessed, it is necessary to assess both. Induced electric field and current density may be measured using the same techniques.

As previously noted, techniques and processes of this type have been created for the compliance testing standards, such as wireless communication devices. These approaches can't be used directly to WPT because of the differing frequency ranges and exposure situations. However, they can provide direction on how to create acceptable procedures for the establishment of a product standard.

2.8 Scope of Hybrid Ray Tracing/Numerical Methods

It is difficult to apply the conventional FDTD method to dosimetry for WPT systems in millimeter frequency range due to the increased number of time steps in wide area. Various exposure scenarios should be evaluated and the fast algorithm will be helpful to process big data. Therefore a Hybrid Ray-tracing with Numerical methods are essential to compute the human exposure evaluation for Wireless Power Transfer for wearable devices and for evaluating the effect of the environment in absorbed electromagnetic energy.

Ray tracing is used to evaluate large regions, whereas FDTD is used to investigate areas near complicated discontinuities when ray-based solutions aren't accurate enough. Because FDTD is only used to a small fraction of the whole modeling environment, the hybrid approach provides enhanced accuracy and practicality in terms of computational resources at the same time.

Combining the Ray-Tracing (RT) for deterministic geometry based propagation calculation and the Finite Difference Time Domain (FDTD) method to assess exposure of a realistic human phantom.

In my thesis we are using mm waves, therefore we are always in far-field region of the source, moreover we can use the core SAR, which is valid up to 300 GHz

Chapter 3

Ray-Tracing and Numerical Methods

3.1 Introduction

Initially, Ray Tracing (RT) models were used in optical propagation issues, based on the ray-optical approximation of the propagation field and the Uniform Theory of Diffraction. It has only been used to forecast radio frequencies for field use in human-made contexts such as indoor and urban environments in the early 1990s, using RT's radio lance, Gausian beam tracing, etc.[2]

While its popularity has grown over years, RT models are still not common in application for the design and planning of mobile radio system issues, largely due to their high calculation time and lack of information and confidence in the environment. Therefore, an important effort in the scientific community dealt with themes such as CPU time reduction by decomposing the 3D problem into 1 or more 2D issues or utilizing algorithm efficiency approaches or simplifying the input data base.

It is likely that things will alter. The development of contemporary broadband, MIMO, beam-forming, and other sophisticated transmission technologies means that the performance of high-speed mobile radio systems no longer rely just on the signals/noises ratio (SNR)[2], but also on the diffuse property of radio transmission. Thus RT models seem to be a suitable option for precise field predictions in site specifications and multidimensional characterisation of the radio propagation channel in time, space and polarisation fields thanks to their inherent capacity to simulate multi-path propagation.

To reach this complete potential, extensions have been recently created to explain diffuse dispersal phenomena to reflect the signal spread in another direction owing to the surface and volume details and imperfections of construction walls in order to fully accomplish this potential.

Future wireless systems will function largely at millimeter wave frequencies because of the higher frequency of the bandwidth available[2]. Due to the very high wall attenuation, the propagation environment at millimeter frequencies is comparatively less than the UHF frequencies, thereby reducing both the input database complexity and the calcular effort. Moreover, the short wavelength makes the ray optical approximation more acceptable compared to the walls and object dimensions and the RT results more accurately.

At the same time, the influence of environmental impacts might grow since even small items could at midwaves serve as a good reflector, creating large multipath contributions at the recipients[2]. Such items should thus be detected and incorporated, in some way, in the digital environment, which, compared to the lower frequency, cannot be described necessarily easier in the end. I hope, that the next future will be more and more accessible to precise digital maps of both outside and even inside areas, as well as inexpensive computer power.

The good prospects for the design, planning and optimisation of the next-generation wireless networks appear to be all regarded RT models. The models of RT have lately been utilized to develop models for the route loss of millimetres[2], frequently combined with measurements, for multidimensional channel characterizations and for the radio interface of 5G mobile radios. Additional current uses include RT for characterizing the Terahertz propagation channel or supporting indoor localization technologies.

3.2   State of Art Techniques for Radio Propagation Model

We will have a glance of the main problems in ray-tracking deterministic propagation modeling in relation to the full three-dimensional (3-D) RT tool developed by the University of Bologna known as 3DScat, along with "standard" interaction measures like "image-RT" reflecting / diffracting / transmission[2].

The usage of an embedded model based on 'Effective Roughness' approach and 'ray launching' technique is taken into account in the Diffuse Scattering (DS). The ER model can represent dispersing events simply yet efficiently owing to wall rough-

ness or imperfections of surface or volume that cannot be described in the input database[2].

Diffuse Scattering (DS) is considered utilizing the embedded model of 'Effective Roughness' (ER) and 'ray launch' method[2]. The ER model may represent dispersing phenomena simply but effectively owing to the raw walls or to abnormalities in surface/volume, which cannot be explained in the data base.

Not with standing an algorithm method, the RT motor must fill the simulation domain with a thorough description of the geometrically and electromagnetically characteristics of each item[2]. The objects are mostly walls, but also pieces of furniture or any other architectural feature or urban furnishings which can occur in or outside of structures. For simplification's sake, a small number of flat surface slab elements are generally considered for each item.. The vertex coordinates, thickness, complex permittivity and diffuse dispersion model parameters of each element should be indicated in the input file. The RT software also needs to include the 3-D polarimetric antenna radiation data[2].

3.3 Sensitivity of RT prediction to environment modeling

The necessity for a very thorough and accurate environment description is an important problem for RT prediction models[2], the more rough and erroneous is the representation of the simulation scenario recorded in the input database(s), the less the forecast accuracy.

Of course, both geometrical and electromagnetic concerns are covered in the environmental description. In all areas engaging with the propagating field, the geometric aspects involve number, form, measurement and location.

Traditionally the essential geometric information was obtained by automated techniques (for instance aerophotogrammetry), which can be rather costly[2]. Nevertheless, open access, digital web-based databases are developing rapidly and this may indicate that in the near future the gathering of geometrical data is to be simplified and made cheaper.

The electromagnetic aspects are related to the evaluation at the frequency of interest of the electromagnetic characteristics (usually confined to the relative permittivity ϵ_r and to the conductivity σ).

3.4   Advanced Applications of Ray Tracing

For the foreseeable future a variety of sophisticated RT applications go beyond the field forecast for radio planning[2]. To meet the growing need for high-performance wireless communication systems in conjunction with the exploitation of new bandwidth at millimeter-wave frequencies, sophisticated radio and antenna technological devices such as MIMO and beam-forming have recently been proposed.

Even if, because of the reduced through-wall penetration, and thus RT application theoretically faster and easier, the spread environment is lower at micro-wave frequencies than UHF, a new difficulty may emerge: due to its low wavelength, even small items not in the environment database can become effective reflectors at midwaves and therefore can make substantial contributions.

One possible solution to this challenge is a description, by means of an experimental characterisation[2], of commonly used items inside the RT algorithm (e.g., neon light mirrors and computer displays) as point scatterers with a typical bi-bistatic radar cross section.

However, this approach requires information of the presence and position of these items and will thus provide new problems for environmental mapping technology.

Another possibility may be the ER model, which might be modified somehow to account for statistically dispersed interior clutters. However, the opportunity to effectively replace small spreaders usually found indoor scenarios with an efficient roughness attributed to the room walls or to other[2], larger objects requires further investigation. This solution should be done without the inclusion of small, dispersive objects in the input database.

Present and prospective millimeter wave applications include indoor gigabit wireless and millimeter front- and rear-wave systems. The short wavelength of millimeter waves permits to employ extremely small beams for high spatial spectrum reuse and signal to interference ratios for large MIMO antennas to use pencil beam formation techniques.

As has already been argued[2], a thin knowledge of the directional properties of the propagation channel might be required to build and optimize systems using such approaches, RT being the ideal instrument for this purpose.

Moreover, the availability in future systems of low-cost computing power, detailed digital 3-D building databases and accurate mobile terminals location techniques will probably promote not merely the use of "offline" RT models to help in systems design and deployment but also to help the system estimate online real-time

channel planning.

Future prospective uses include embedded real-time applications for optimum beam-forming or beam switching techniques for mobile back-hauling systems (MBH, also known as mobile front hauling) or for multi-giant wireless applications[2]. Radio frequency patterning or radio location printing methods are some approaches where RT might soon be successful.

Chapter 4

Models and Methods

4.1 Introduction

The Finite-Difference Time-Domain (FDTD) approach is now the most widely used method for assessing the power absorbed in a subject exposed to EM fields. When modeling exposure in an urban context, however, the FDTD is difficult to utilize due to the large size of the region to be analyzed in comparison to the typical wavelength employed in cellular telecommunication networks.

FDTD method can be used to study a limited region just containing the exposed subject, and geometrical optics is used to model the field propagation in the remaining part of the domain, including the radiation antenna and the reflecting/scattering objects. The radiation pattern of the antenna, which is the input of the hybrid method, has been computed by means of FDTD analysis.

4.2 Models and Methods

In electro-magnetic dosimetry difficulties, the FDTD approach is now the most often used methodology[18]. In fact, it enables a sufficiently precise simulation of the field source (antenna) as well as a straightforward modeling of heterogeneous scatterers with various shapes(human body).

Due to the massive memory and CPU time requirements, this approach is ineffective for studying scattering issues involving vast areas (urban environment). To solve this challenge, the FDTD approach has combined with the Ray-Tracing methodology in this research, which is capable of modeling field propagation in huge multi-reflection settings relatively effectively.

the following are been discussed

1. Numerical Pipeline

2. Ray tracing simulation
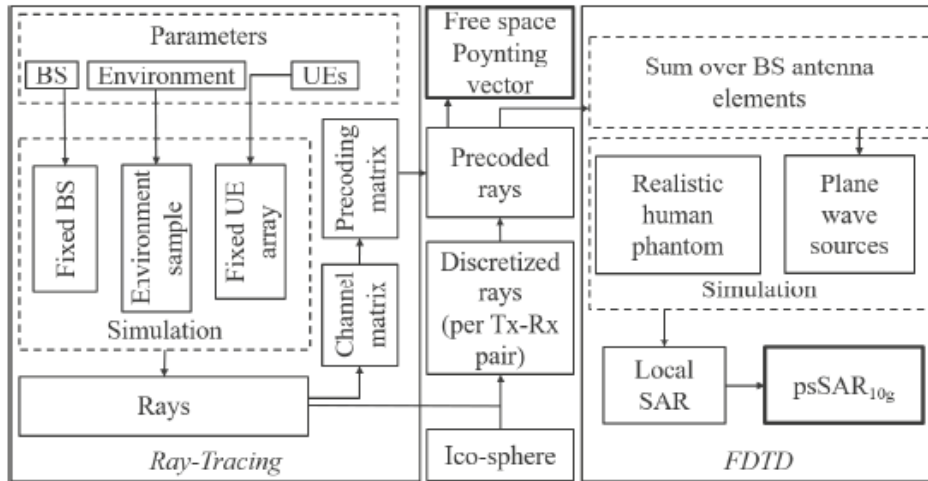
Figure 4.1: Numerical pipeline scheme. Ray-tracing, FDTD and the interface between them)[2]

4.2.1   Numerical Pipeline

When analyzing exposure statistically [18], one approach to do this is to use a known DoA distribution for a certain kind of environment.

Because the input to a RT simulation is a geometrical model of an environment, the RT technique offers the following benefit over stochastic models: instead of being sampled stochastically[18], all channel information is retrieved from the environment model. The definition of the RT simulation domain is comparable to the selection of distribution parameters in a stochastic model.

The incidence directional information at the Receiver is spatially consistent. Between the Transmitter and Receiver, scatterer clusters arise naturally as the strongest propagation pathways. Importantly, RT estimates DoA for each individual Receiver depending on the antenna array's geometry, direction in space, and other factors. The length of the propagation channels (path loss), probable reflections, transmissions (Fresnel equations), and diffraction's that a ray experiences throughout its passage are used to compute the power distribution, phase, and time-delay of incoming beams.

Antenna radiation patterns are simple to include in RT simulations because scaling the incident power with respect to direction of departure (DoD) at the transmitter and direction of arrival (DoA) at the receiver is all that is required; this can be done as a post processing step of simulation results.

4.2.2 Ray-Tracing Simulation

The ray-tracer [18] calculates the channel transfer function between the nth Transmitter and the kth Receiver given that the Transmitter are stimulated with a sinusoidal signal at frequency f_c.

$$h_k^n = \sum_{r=1}^{s(k,n)} p_r exp(-2\pi i f_c \tau_r) \tag{4.1}$$

where s(k,n) denotes the total number of pathways found between the nth Tx and the kth Rx locations, p_r denotes the complex-valued impulse response along the rth path, and τ_r denotes the rth path's time delay.

4.3 RAY-TRACING and FDTD

The ray-tracing technique, which is based on geometrical optics (GO) and is frequently augmented with the uniform theory of diffraction (UTD)[19] , gives a reasonably straightforward solution to indoor radio propagation. However, it is commonly understood that GO produces good results for electrically big objects, but UTD is only stringent for completely conducting wedges. Ray tracing fails to anticipate the dispersed fields accurately for complicated lossy objects with finite dimensions found in an indoor setting.

Transmitting and receiving antennas are frequently deployed close to these complex discontinuities in the challenging interior communication environment[19] , where no asymptotic solutions are accessible. The numerical solution of Maxwell's equations, namely the finite-difference time domain (FDTD) approach, can be used to address such a problem.

The FDTD approach completely accounts for the effects of reflection, diffraction, and radiation by directly solving Maxwell's equations in the time domain[19]. The medium constitutive relation is automatically integrated into Maxwell's equation solutions. As a result, it is ideally suited to investigating wave interactions in complicated media. The precision of the FDTD approach, as well as the fact that it

simultaneously offers a full solution for all locations on the map, allows it to deliver signal coverage information over a given region.

However, being a numerical analytic approach, the FDTD method necessitates a substantial amount of memory to maintain track of the solution at all locations, as well as intensive calculations to update the solution at consecutive time instants. Because of the processing resources required, applying an accurate numerical analysis approach to the full modeling area is not possible nor essential for open spaces with few indoor items.

The core concept is to utilize ray tracing to examine large regions and FDTD to research areas near to complicated discontinuities where ray-based solutions are not precise enough. FDTD is only applied to a tiny section in our case the Human body of the total modeling environment, ensuring computational resource efficiency.

The proposed hybrid technique allows for the investigation of the impacts of general interior structural characteristics, furniture, inhomogeneity inside walls, and any other things that may have a major impact on field strength levels inside the human body.

In the FDTD computation domain, signal intensity and phase at all places may be acquired.

Ray tracing is originally used to cover a vast region with huge scale and weak inhomogeneities. Objects are represented as dielectric slabs with predetermined thickness, boundaries, dielectric constant, and loss tangent, which is suitable for most interior barriers such as walls, ceilings, floors, windows, and doors. The coefficients of reflection and transmission for lossy dielectric slabs are calculated. Another propagation process used in ray tracing is diffraction. Most diffraction-causing structures in an interior setting may be divided into two types: thick half planes such as doors, windows, and partitions, and right-angle wedges such as wall corners.

4.4   3D-SCAT

3DScat is a deterministic field prediction program based on geometric propagation theory.

The software functions in two different and sequential phases, beginning with an acceptable description of the propagation environment, moving on to the position of the transmitter (Tx) and receiver (Rx), and the radiation parameters of the antennas.

Calculation of optical ray paths between Tx and Rx using geometric optics (GO) principles and extensions (Uniform Theory of Diffraction - UTD - and diffuse scattering models);

Calculation of how the field evolves as it propagates along the rays, as well as evaluation of the consequences of received multipath (in terms of received power, power delay profile, delay and angular spread, and so on).

The software must fundamentally understand:

- The propagation scenario, that is, what objects may interact with the radio signal and how they are formed (size, shape, component materials).

- The position of the transmitter / receiver and the radiation parameters of the antennas employed.

The propagation environment is primarily specified by two ASCII files :

- filename.data

- filename.list

- **Filename.data**

  Essentially, it depicts the "things" encountered in the propagation environment geometrically (in most cases, the walls). The total number of walls is the first data point in the file, followed by a geometric description of each of them.

  These are flat polygons with four vertices (in reality, rectangles or triangles if two points are coinciding), which are therefore uniquely specified by assigning the coordinates of the vertices (12 bits of information) with regard to a particular reference system (hence it). It shall be referred to as "absolute reference" or "environmental reference" in the following; the walls might be vertical, horizontal, or oblique.

  Unless you want the described wall to reflect on one side only (for example, a perimeter wall that delimits the simulation environment), the vertices must be specified so that the normal to the wall (in the half-space of reflection) "sees" the vertices assigned in an anticlockwise direction.

  The walls can be vertical, horizontal, or slanted in any direction. Unless you want the described wall to reflect on one side only (for example, a perimeter wall that delimits the simulation environment), the vertices must be specified

so that the normal to the wall (in the half-space of reflection) "sees" the vertices assigned in an anticlockwise direction.

Moreover, each wall is followed by a progressing natural identifier (order number) and a string that specifies "the kind of wall" (through the identifier in the.list file, its features in terms of parameters are connected with each wall electromagnetic characteristics, thickness,"bilateral," etc.).

Following the description of the walls, it is important to include in the file a list of the diffraction edges in an acceptable manner (geometrically they are segments). In the case of walls, first indicate the total number of edges, followed by a description for each of them, assigning the following parameters: a progressive identifier, the coordinates of the two extremes (6 values), the identifiers of the two walls that intersect and identify the corner, and the angular width of the corner.

In terms of breadth, the literature is consulted, and the angle to be regarded is that in the "full" of the wedge; with an angle equal to zero, an edge is indicated, that is, a diffracting half plane; in this instance, the two walls plainly coincide.

Lastly, 3DScat allows you to define discontinuities in the walls, such as "holes" that symbolize doors and/or windows. Discontinuities, by definition, are always and only rectangular, and they always affect both sides of the wall (paintings on a wall, for instance, cannot be defined as discontinuities).

The .data file then concludes with a description of the (possible) discontinuities: after indicating the total number of discontinuities, each one is described by a progressive identifier, the coordinates of two opposite vertices of the rectangle that geometrically describes the discontinuity, the identifier of the wall to which it belongs, and finally a string that defines (in the.list file) the type and properties of the discontinuity (properties that differ from those of the wall in general, both in terms of EM parameters and traversability).

- **filename.list**

    It provides specific characteristics to be associated with the object to which the string refers for each of the "type strings" used in the .data file. These parameters, in particular, are the relative permittivity (ϵ_R.), conductivity (σ), thickness, and whether or whether the wall is permeable and is

bilateral or less. Furthermore, for each type of wall, precise values of the scattering parameter, both backward (S_R) and forward (S_T), can be specified as optional options. If S_R and S_T values are not supplied, the default values are used, which are specified together with the other input parameters.

There are three ASCII files (run name.rays, run name.pow, and run name.pdp), plus an extra file (run name.mr) if the SAVE MR flag in the param.dat file is set to 1. These files are discussed briefly below.

- **run_name.rays**

  The run_name.rays represents the rays that have been discovered between Tx and Rx (based on the constraints provided in the control string). Each ray is envisioned as a broken line and then defined by sequentially assigning the coordinates (x, y, z) in the environment. Obviously, the start and final points of each line coincide with Rx and Tx locations, respectively.

- **run_name.pow**

  It describes the received signal strength, the channel transfer function (between the terminals of the transmitting and receiving antennas), the value (complexity), and the polarization of the "total field received" (meaning the field that would exist in the absence of the receiver) for each receiver.

- **run_name.pdp**

  It highlights the key properties of each ray, such as the series of interactions, departure / exit angles, latency, polarization coefficient, strength, incident field connected with the ray, and so on.

- **run_name.mr**

  It is only produced if the MAKE MR flag is set to 1. In fact, the .mr file includes roughly the same information as the .pdp file but has been "reordered" in matrix form so that it can be fed into Matlab (through the GetData.m script) and utilized by post-processing filters.

Chapter 5

Results

The aim of the work is to identify the sensitivity of the absorbed electromagnetic energy of a wearable WPT device, with respect to the environment, the receiver position, the antenna orientation through a hybrid 3-D ray tracing/FDTD tool. A Hybrid RT-FDTD solution is proposed which is able to account for the environmental characteristics (presence of furniture, windows, doors, etc...) and for the characteristics of the human body (anatomy, electromagnetic characteristics of the biological tissues, etc..).

In this work we have combined the hybrid RT with a FDTD method. A brief overview of hybrid Ray-Tracing/FDTD methods regarding the improvements with regard to techniques available have already been discussed in the previous chapter, while in this chapter integrate RT is integrated with FDTD to complement optimum evaluation of human exposure for wearable wireless power transfer devices.

5.1 The tested environment

The working frequency has been set to 28 GHz as one of the frequencies that have been auctioned for 5G. The environment where simulations have been performed in order to check the reliability of the whole process is shown in figure 5.1, it is a typical office, with windows, cupboards and a person wearing the wearable WPT device on his arm. Firstly, the transmitter is set in one corner of the room at 2.5 meters height, and different receiver locations, displaced on a plane at 1.5 meters from the floor are considered.

The Tx is an omnidirectional antenna in order to radiate with the same intensity in every direction, while the Rx antenna is a directional antenna, especially conceived

Simulation environment
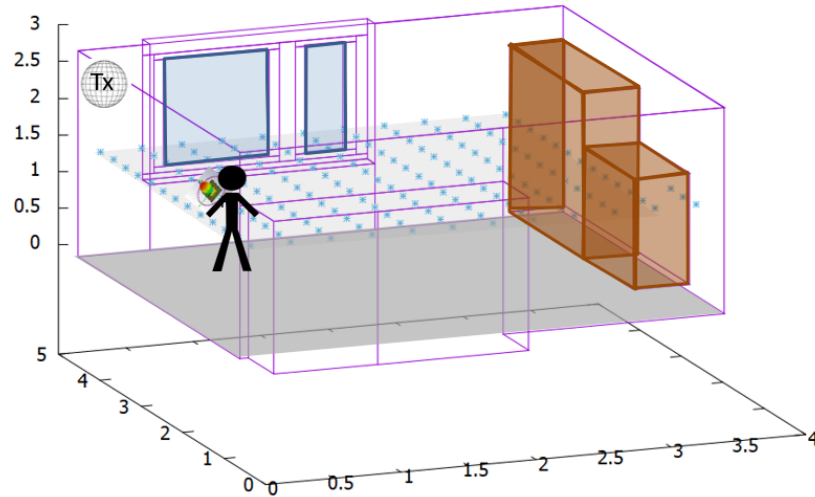
Figure 5.1: Simulation Environment

for the wearable WPT device, in figure 5.2 the 3D radiation diagram of the Rx antenna is presented.
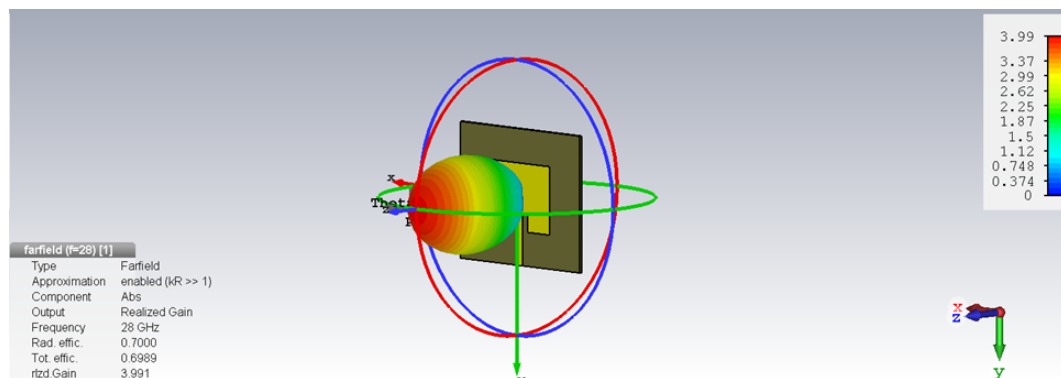
Figure 5.2: 3D radiation diagram of the Rx antenna

For each receiver location field strength levels have been evaluated and simulations have been performed with different orientation of the receiver antenna: Rx oriented to the direction of the receiver antenna, then rotated of $90°$, $180°$ and $270°$ with respect to the LOS with the Tx. As from the output field strength levels are very weak in general and when the Tx is not facing the transmitter field strength

levels drop down to -90 dBm, which it may be below the sensitivity of the receiver.
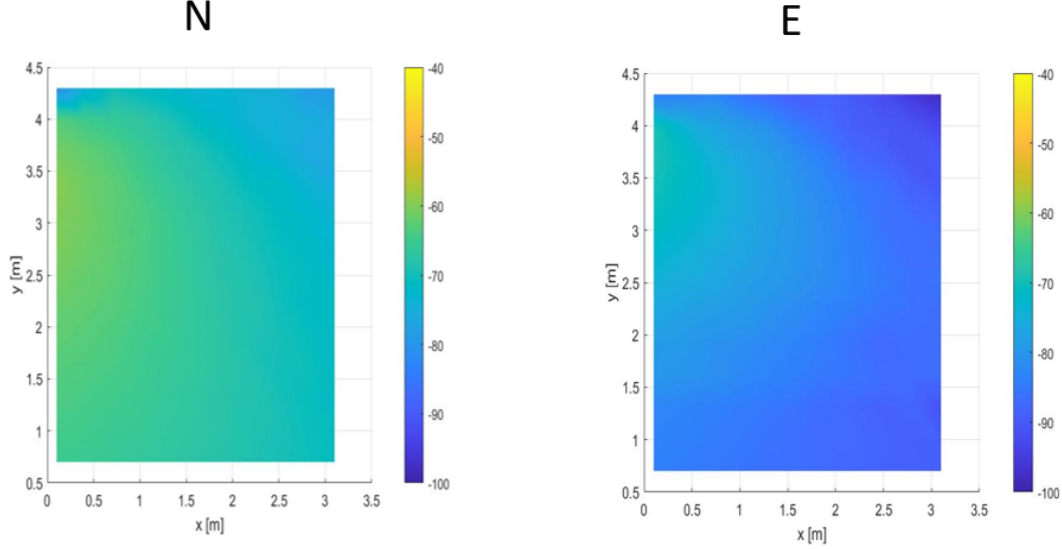
Figure 5.3: Received power for all the receiver positions and for two different antenna orientations

From figure 5.3 is clear that the distance from Tx to Rx should be very small in order to get the sufficient energy to efficiently power the device wirelessly. As a matter of fact it is well known that free space attenuation @ 28 GHz is very high:

$$FSL \text{ @ } 1 \ m = 20 log_{10} \left(\frac{4\pi d}{\lambda} \right) = 61.38 \ dB \qquad (5.1)$$

$$FSL \text{ @ } 0.5 \ m = 55.36 \ dB \qquad (5.2)$$

To better highlight field strength level distribution in the simulated environment in Figure 5.4 the Cumulative Distribution Function of the received power for different receiver directions is shown. The CdFs for different orientations of the receiver show that as soon as the RX is not facing the Tx, the received power drop down of about 15 dB (from -68 dB for the mean value of the receivers facing the Tx to -82 dB of the mean value for the receivers of the South orientation). It is interesting to highlight that the South orientation perform better in terms of received power (at least up to the 70% of the receivers locations) with respect to the East and West orientation. This behaviour may be due to the influence of the environment, the South oriented receivers can take advantage of a higher number of reflections in the South wall.

In order to further investigate the effect of the environment on the receiver field strength level we move the Tx to a lower height (at the same height of the Rx), to
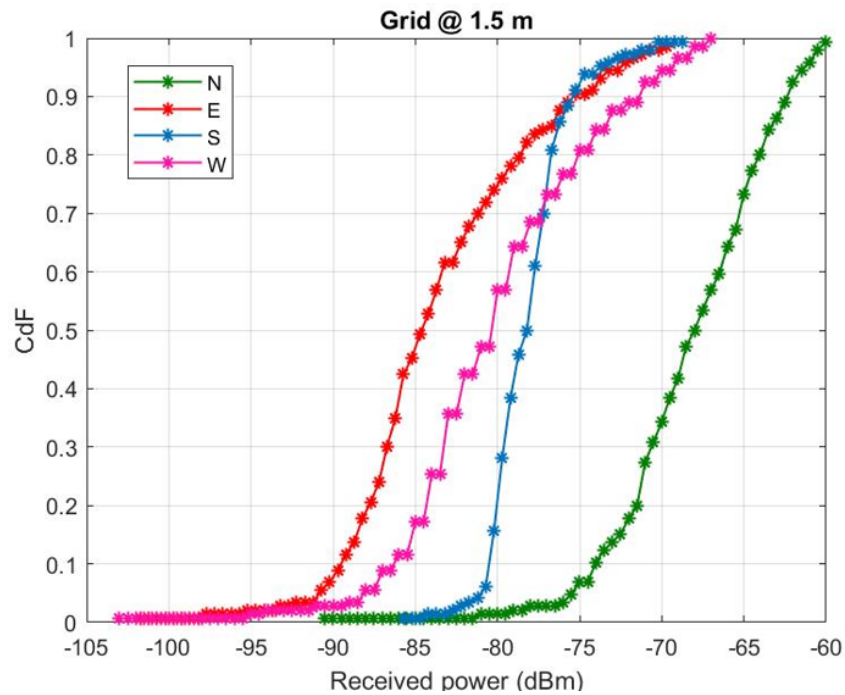
Figure 5.4: Cumulative Distribution Function Of Rx Power
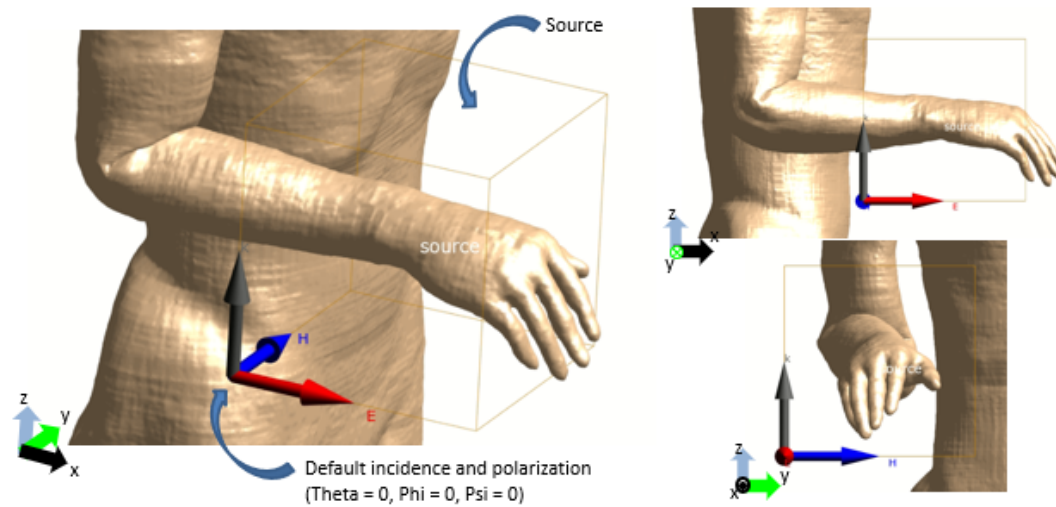
Figure 5.5: source of a plane wave is rectangular in shape, originating on the lower right vertex of the rear face

decrease the FSL.

We can see from the figure 5.6 (left) that, lowering the Tx height yields to an overall increase of the received power. This is clear from the CdFs (Figure 5.6 right orange line) where a shift of 4 dB of the North orientation with a lower height is
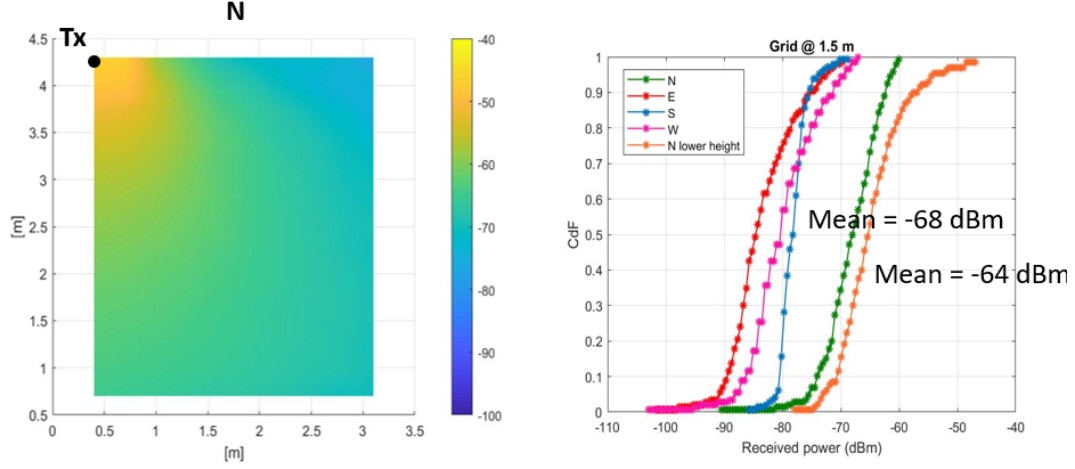
Figure 5.6: Tx and Rx at the same height

observed. To conclude, due to the high FSL, the orientation of the Rx antenna and the influence of the environment, the receiver have to be close to the transmitter to receive the sufficient energy to feed the wearable WPT device.

As we would be close to transmitter for sufficiently feeding the WPT Device we have to evaluate the absorbed energy into the human body and check compliance with the international ICNIRP Guidelines. To this aim we use the output of the RT tool as the input for the FDTD simulation Sim4Life [Sim4Life] which is a simulation platform, combining computable human phantoms with the most powerful physics solvers and the most advanced tissue models, for directly analyzing biological real-world phenomena and complex technical devices in a validated biological and anatomical environment. In Sim4Life the simulation domain is always a rectangular domain, originating on the lower right vertex of the back face as observed in figure 5.7.

In Sim4Life the source is a plane wave, originating on the lower right vertex of the rear face as seen in figure 5.5. In order to account for the multipath in the environment and make the simulation closer to reality, the possibility to feed Sim4Life with a higher number of plane waves (as output of the RT tool) has been investigated.

As input Sim4Life needs the amplitude of the field, the direction of incidence (θ,ϕ) of the wave in a polar reference system and the polarization angle (ψ) of the field, according to the circular polarization decomposition. In the figure 5.8, the aforementioned angles are reported:

The reference system is taken into account in polar coordinates, so the angles of
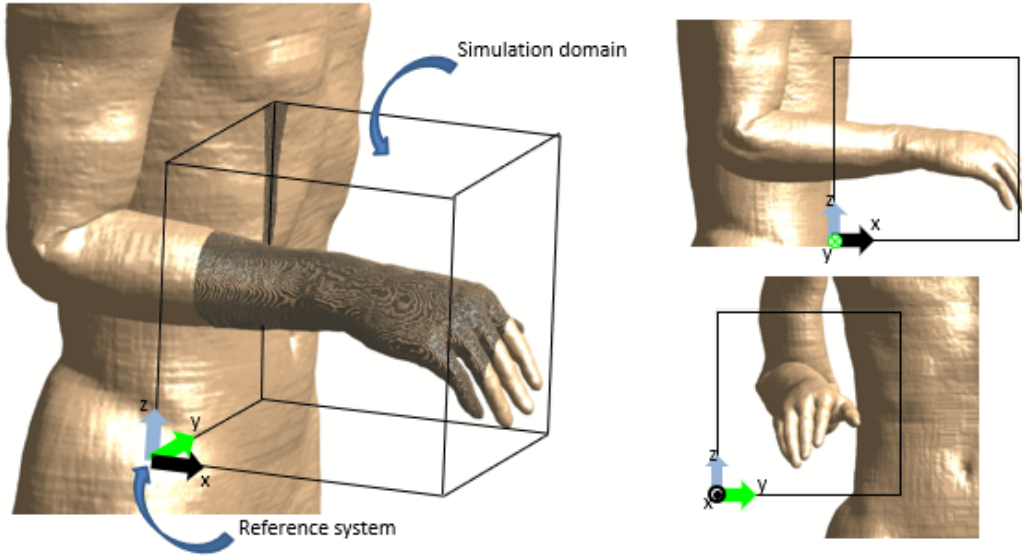
Figure 5.7: A rectangular simulation domain domain, originating on the lower right vertex of the back face

θ: elevation of the propagation vector k.

φ: azimuth of the propagation vector k.

Ψ: polarization angle.
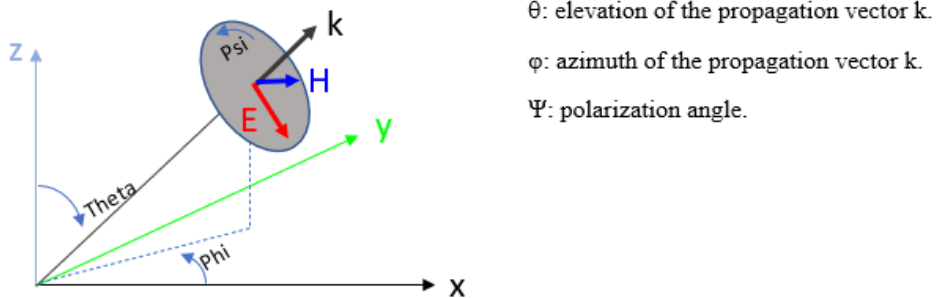
Figure 5.8: Graphical Representation of θ,ϕ,ψ angles

the direction of incidence (θ,ϕ) and the polarization (ψ) are given in polar coordinates, with the following ranges: $0°<\theta<180°$, $0°<\phi<360°$, $0°<\psi<360°$. According to the requirements of S4L we have provided the theta(θ), phi(ϕ),and psi(ψ) values for a certain number of plain waves, each plane wave is represented by a ray which is the output of the RT tool.

If we consider the tested scenario of Figure 5.9 for instance, and according to the reference system S4L needs, we have selected the 3 strongest rays in the environment as shown in Figure 5.10. For each of the selected rays, e.g. the direct ray in the Figure 5.10 (ray n. 1), the received power, the direction of incidence angles (θ,ϕ) and the polarization (ψ) are given as defined in S4L and within the allowable ranges.

(a) Side View

(b) Top View

Figure 5.9: Simulation Environment

Figure 5.10: Selection of 3 strongest Rays

Table 5.1 gives the data of the 3 strongest rays with their respective angles. The test simulation was set with the aim of having the electric field with component only along phi (in polar coordinates)/along y (in cartesian coordinates), being the Tx and Rx at the same height, theta is always 90 degrees since the ray (therefore the propagation direction) always belongs to a plane parallel to the xy plane. In the right figure 5.10 the selected rays are shown according to the reference system of S4L.

RAY NO	THETA	PHI	PSI	Received Power
1	90°	180°	90°	-64.9069 dBm
2	90°	99°	270°	-103.871 dBm
3	90°	329.47°	90°	-114.171 dBm

Table 5.1: Selected Rays According to Their Received Power

In the following figures an example of the output of S4L is shown for the combination of 2 rays [20]
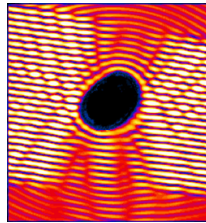
Figure 5.11: Transverse plane (XY) passing through the wrist
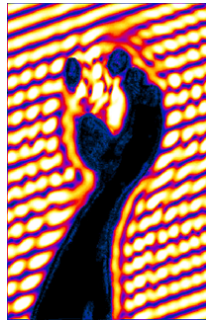
Figure 5.12: Axial plane (YZ) passing through the centre of the hand
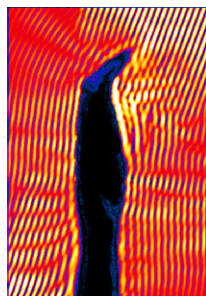
Figure 5.13: Longitudinal plane (XZ) passing through the centre of the hand

Chapter 6

Conclusions

Wearable Wireless Power Transfer devices are becoming more and more widespread as remote health control systems that allows patients for home monitoring, enables better life and more sustainable health care systems. Specifically, in this work the far-field radiative coupling mechanisms for WPT in the millimeter (mm)-wave range has been considered, which has not been intensively studied so far for WPT applications, due to the inherent high free space loss, but it is currently under vast investigation as the future EM spectrum for the development of 5G communications.

In this framework the evaluation of human exposure to has become an important issue. As a matter of fact, these devices usually operate in indoor, in a rather complex environment where scattering objects are present, which can influence the received power level by means of reflections, diffractions and scattering. In these situations, accurate investigations are needed to assess if human exposure can give rise to health risks and to verify compliance with the existing protection standards.

In this work, the exposure of a subject, a realistic human phantom, to the field received by the wearable WPT device in an indoor environment has been studied. The exposure has been analysed coupling the FDTD method, which is able to evaluate the SAR Specific Absorption Ratio value inside the human body, with a ray-tracing algorithm, suitable to assess field propagation in furnished indoor environment and accounting foe all the possible interactions with the objects in the environment. The obtained results show the possibility of highlighting possible non uniformity of the field distribution due to the presence of different objects in the environment.

The introduced approach can be further extended considering other types of environments (e.g. outdoor) and topologies. Moreover, thanks to the hybrid method (RT/FDTD) the effect of different propagation mechanisms on absorbed energy

inside the human body can be investigated. This remains to be the main focus of the future research.

Bibliography

[1] "Overview Â» it'is foundation," `https://itis.swiss/virtual-population/virtual-population/overview/`, (Accessed on 09/23/2021).

[2] Franco Fuschini, Enrico M. Vitucci, Marina Barbiroli, Gabriele Falciasecca, and Vittorio Degli-Esposti, "Ray tracing propagation modeling for future small-cell and indoor applications: A review of current techniques," *Radio Science*, vol. 50, no. 6, pp. 469–485, 2015.

[3] Andreas Christ, Mark Douglas, Jagadish Nadakuduti, and Niels Kuster, "Assessing human exposure to electromagnetic fields from wireless power transmission systems," *Proceedings of the IEEE*, vol. 101, no. 6, pp. 1482–1493, 2013.

[4] Lijia Zhu, Huan-sheng Hwang, Eugene Ren, and Guangli Yang, "High performance mimo antenna for 5g wearable devices," in *2017 IEEE International Symposium on Antennas and Propagation USNC/URSI National Radio Science Meeting*, 2017, pp. 1869–1870.

[5] "Wearable technology definition," `https://www.investopedia.com/terms/w/wearable-technology.asp`, (Accessed on 08/14/2021).

[6] "(pdf) evolution of wearable devices with real-time disease monitoring for personalized healthcare," `https://www.researchgate.net/publication/333472144_Evolution_of_Wearable_Devices_with_Real-Time_Disease_Monitoring_for_Personalized_Healthcare`, (Accessed on 09/09/2021).

[7] "The history of wearable technology - blog," `https://www.condecosoftware.com/blog/the-history-of-wearable-technology/`, (Accessed on 09/30/2021).

[8] Guoguang Rong, Yuqiao Zheng, and Mohamad Sawan, "Energy solutions for wearable sensors: A review," *Sensors*, vol. 21, no. 11, 2021.

[9] "Panasonic high-temperature long-life nickel metal hydride battery," `https://www.designworldonline.com/panasonic-high-temperature-long-life-nickel-metal-hydride-battery/`, (Accessed on 09/12/2021).

[10] "Sensing an opportunity for indoor pv â pv magazine international," `https://www.pv-magazine.com/2019/07/17/sensing-an-opportunity-for-indoor-pv/`, (Accessed on 09/12/2021).

[11] "Flexible thermoelectric generator module: a silver bullet to fix waste energy issues," `https://phys.org/news/2018-12-flexible-thermoelectric-module-silver-bullet.html`, (Accessed on 09/12/2021).

[12] Young-Man Choi, Moon Gu Lee, and Yongho Jeon, "Wearable biomechanical energy harvesting technologies," *Energies*, vol. 10, no. 10, 2017.

[13] "Electronic skin fully powered by fuel cells and sweat can monitor health - fuelcellsworks," `https://fuelcellsworks.com/news/electronic-skin-fully-powered-by-fuel-cells-and-sweat-can-monitor-health/`, (Accessed on 09/12/2021).

[14] "Magnetoelectric wireless power transfer for biomedical implants: Effects of non-uniform magnetic field, alignment and orientation - sciencedirect," `https://www.sciencedirect.com/science/article/abs/pii/S0924424720308967`, (Accessed on 09/12/2021).

[15] "Safe for generations to come," `https://www.ncbi.nlm.nih.gov/pmc/articles/PMC4629874/`, (Accessed on 09/12/2021).

[16] "Icnirprfgdl2020.pdf," `https://www.icnirp.org/cms/upload/publications/ICNIRPrfgdl2020.pdf`, (Accessed on 11/26/2021).

[17] "Iec 62311:2019 - assessment of electronic and electrical equipment related to human exposure," `https://standards.iteh.ai/catalog/standards/iec/72d62d99-6449-44b9-925a-77fce9236723/iec-62311-2019`, (Accessed on 09/20/2021).

[18] Sergei Shikhantsov, Arno Thielens, GÃ¼nter Vermeeren, Emmeric Tanghe, Piet Demeester, Luc Martens, Guy Torfs, and Wout Joseph, "Hybrid ray-tracing/fdtd method for human exposure evaluation of a massive mimo technology in an industrial indoor environment," *IEEE Access*, vol. 7, pp. 21020–21031, 2019.

[19] Ying Wang, S. Safavi-Naeini, and S.K. Chaudhuri, "A hybrid technique based on combining ray tracing and fdtd methods for site-specific modeling of indoor radio wave propagation," *IEEE Transactions on Antennas and Propagation*, vol. 48, no. 5, pp. 743–754, 2000.

[20] "Sim4life Â≫ zurich med tech," `https://zmt.swiss/sim4life/`, (Accessed on 01/28/2022).

Acknowledgements

I would like to express my sincere gratitude to my supervisor, Prof. Ing. Marina Barbiroli and Prof. Ing. Franco Fuschini for giving me this opportunity to do this research and providing integral guidance throughout this research. It was a great privilege and honor to work and study under their guidance. I am extremely grateful for what they have offered me.

I would like to thank my Senior Mr.Swapnil S. Shinde and my Dearest friend Mr.Raja Rohit Poluru for their time and constant support throughout the thesis. I cannot describe their support in words except that I could not have imagined having a better guidance for my thesis.

I would like to thank the program coordinator Giulio Ascari for accepting my admission in to this wonderful university which changed my career and all the professors and staff in the Department of Telecommunications for their effort and kindness during these years.

I thank my parents and my brother for all the moral support they gave me during these 3 years and my friends and roommates who have been there for me in all my ups and downs.

At last, I am grateful to all those people who have supported me to complete my thesis directly or indirectly.

<div align="right">. . . Girish Satya Bhargav Papolu</div>